

DESCRIPTIVE ANALYSIS OF MASSES OF OCEAN WATER THAT ARRIVE TO THE GULF OF MEXICO

Alberto Mariano Vázquez de la Cerda

INTRODUCTION

The ocean is composed of different water masses that normally have layers of lower density water on the surface and higher density water on the bottom. Water masses are formed on the surface due to temperature reductions and/or increases in salinity, therefore they sink until they arrive at equilibrium. Generally, reduction in the temperature of the sea is due to cold atmospheric fronts that take heat from the surface. Increases in salinity are a result of evaporation; the dissolved salts do not evaporate with the water thus salinity rises. This happens mainly in middle latitudes of the Earth where climate zones with high atmospheric pressure are found. In the case of both temperature reduction and increased salinity, density of seawater increases and it sinks as a result.

Physical oceanography uses the T-S diagram (temperature versus salinity) to understand the characteristics and the density of seawater (ρ). In these diagrams, a point indicates a type of water, whereas a line corresponds to a mass of water. The techniques used by physical oceanographers detect the most prominent water masses with maximum and minimum values for temperature and salinity. Some parameters, such as dissolved oxygen and nutrients (mainly silicates and phosphates), which are included in the T-S diagram, are also indicators of different water masses.

There are six regions where water masses are formed in the Atlantic Ocean

1. The Labrador Sea in northeastern Canada and southeastern Greenland.
2. The Greenland and Norwegian seas between Iceland, Greenland and Norway.
3. The western Sargasso Sea and the southeastern Gulf Current in the north Atlantic.
4. Southeastern Brazil in the south Atlantic.
5. The southern south Atlantic between the polar fronts.
6. The Weddell Sea in Antarctica.

The deep waters of the Atlantic Ocean are formed in the regions A, B and F; the water mass called 18°C Sargasso Sea Water (18SSW) is formed in the region C; the water mass called South Atlantic Central Water (SACW) is formed in the region D; and finally, the water mass called Antarctic Intermediate Water (AAIW) is formed in the region E. The last three water masses arrive to the Gulf of Mexico via the Atlantic Ocean (Fig. 2.1).

18°C SARGASSO SEA WATER (18SSW)

The changes in the characteristics of the 18SSW are part of the climatic changes in the north Atlantic. The surface temperature of the sea is an indicator of climatic change in all the northern Atlantic and varies over long periods as has been demonstrated by Bjerknes (1964) and Colebrook and Taylor (1979).

In 1959, Worthington suggested that the 18SSW, formed in the western north Atlantic Ocean and immediately to the south of the Gulf Current (Fig 2.2), is produced in a similar manner to the water on the ocean floor in high latitudes. That is to say, in autumn or winter when atmospheric cold fronts have passed and sea surface temperatures decrease and density increases,

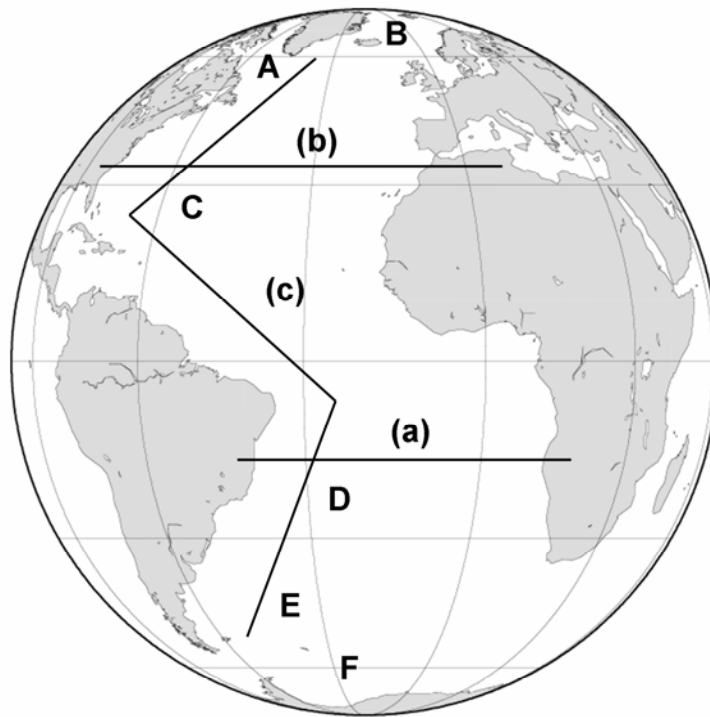


Fig. 2.1. Location of the regions in the Atlantic ocean where water masses form. Three of these water masses (C, D, E) move into the Gulf of Mexico. A = Labrador Sea; B = Greenland Sea and Sea of Norway; C = western Sargasso Sea; D = southeastern coast of Brazil; E = zone between polar fronts in the southern South Atlantic; F = Weddell Sea. Salinity along transect (c) is shown in Figure 2.3. Salinity profiles along transects (a), (b), and (c), are shown in Figure 2.13.

surface water masses sink until they reach equilibrium and remain between denser waters below and less dense waters above. Excessive quantities of the water mass cool and it sinks and starts to flow southwards. Warmer waters that flow northwards by advection then occupy the space left by the sunken water. In the case of 18SSW, the main thermocline is analogous to the sea floor in high latitudes.

There are two masses of water in the north Atlantic that are formed by convection in winter, the 18SSW (Fig. 2.2) in the western north Atlantic (Worthington, 1959), and the North Atlantic Deep Water (NADW; Fig. 2.3). Both are characterized by vertical homogeneity during the whole year because their origin is convective. The 18SSW is formed southeast of the Gulf Current and is found in the center of the subtropical gyre in the western north Atlantic.

Figure 2.4 shows the superficial salinity and clearly shows the ocean gyre nucleus with maximum salinity in the north Atlantic, with values greater than 37.25 PSU. The 18SSW, located between the southeastern Gulf Current and the extreme north of the nucleus of high salinity, and is nearly 200 m thick due to its convective origin. The nucleus was identified using the method

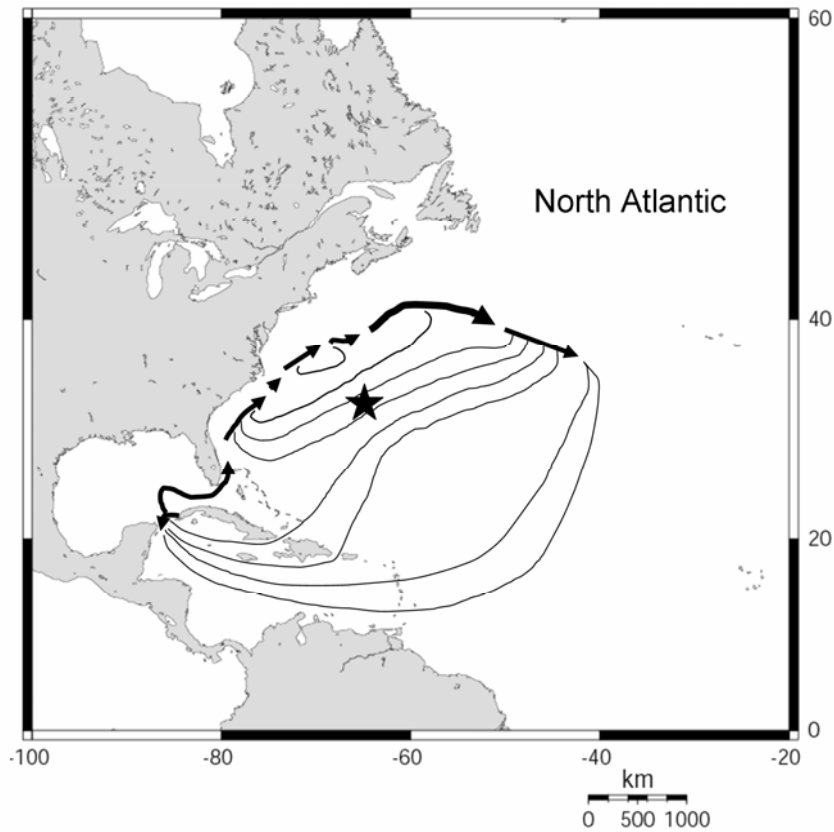


Figure 2.2. Circulation of warm water ($> 17^{\circ}\text{C}$) in the North Atlantic according to Worthington (1976). The black star indicates the position of the station Panuliris ($32^{\circ} 10' \text{ N}$, $64^{\circ} 30' \text{ W}$). Redrawn from Tally and Raymer (1982).

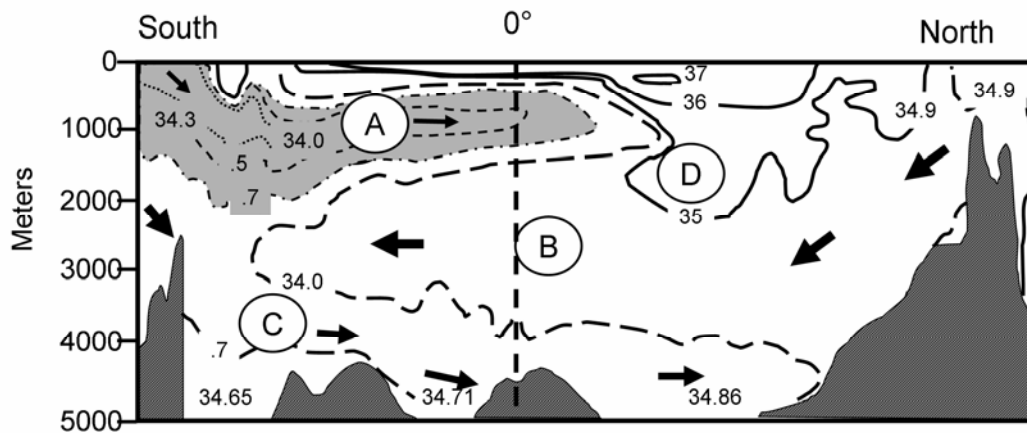


Fig. 2.3. North-south vertical salinity profile (PSU) in the western Atlantic Ocean. Redrawn from Wüst (1935). A = Antarctic Intermediate Water (AAIW); B = North Atlantic Deep Water (NADW); C = Antarctic Bottom Water (AABW); D = Mediterranean Water (MW).

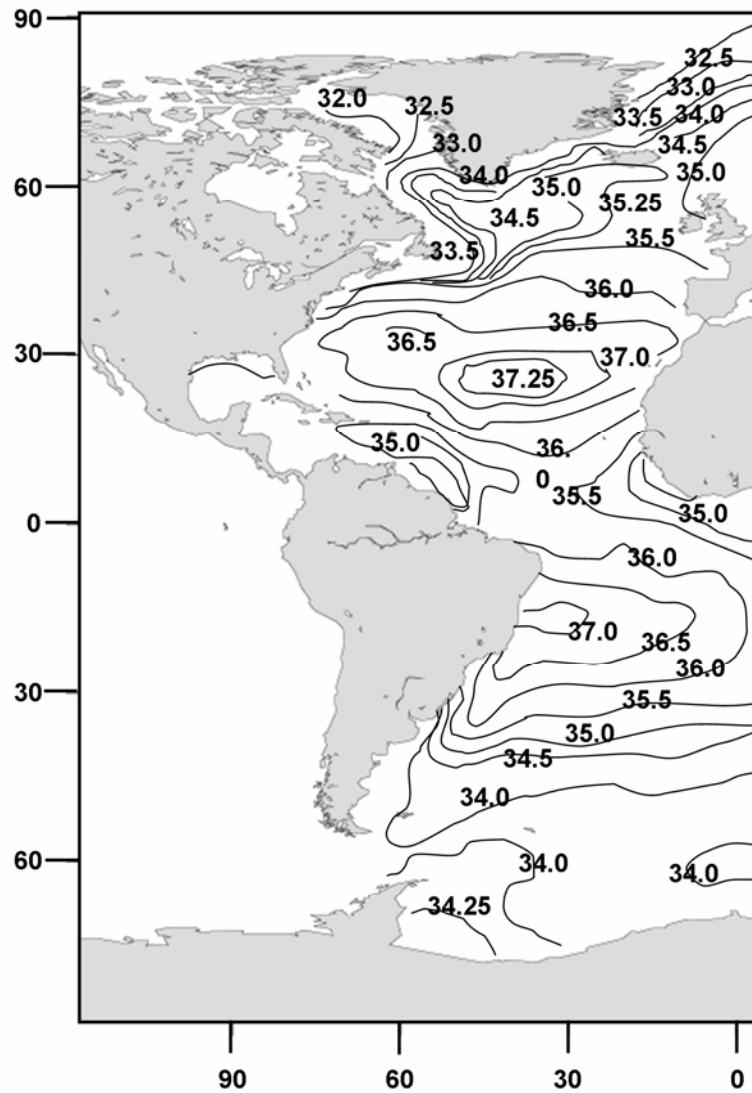


Fig. 2.4. Surface salinity (PSU) in the Atlantic Ocean.

developed by Talley and Raymer (1982). Worthington (1959) defined 18SSW by the temperature at $17.9^{\circ}\text{C} \pm 0.3^{\circ}\text{C}$, $S = 36.50 \pm 0.10$ PSU and $s_t \sim 26.4 \text{ mg cm}^{-3}$ (Figs. 2.5 and 2.13b). The greatest depth of the main thermocline, found to the south of the Gulf Current, is *always* below the deepest part of the mixing layer of 18SSW. This maximum depth of the thermocline represents the center of the anticyclone ocean gyre in the north Atlantic.

The 20-year cooling period at the beginning of the 20th century that was followed by a period of warming in the 1930s was directly related to wind changes (Bjerknes 1964). This author showed that strong trade winds were correlated with a reduction in the sea surface temperature in the Sargasso Sea, and an increase in the surface temperature of the water on

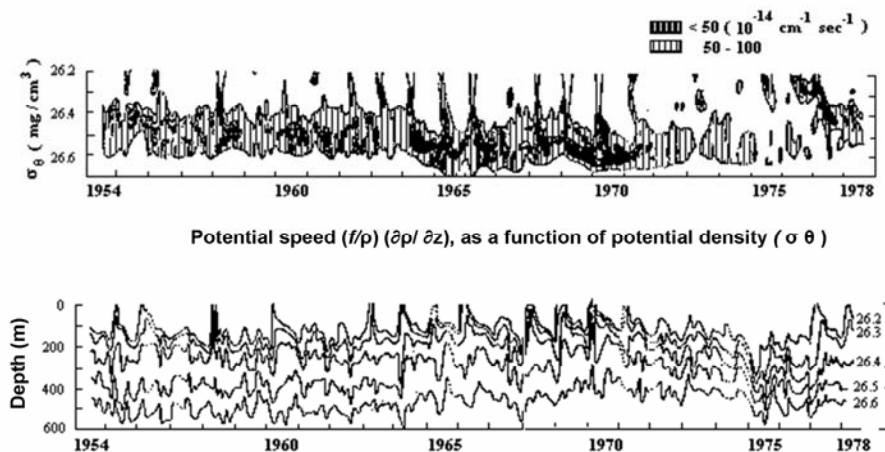


Fig. 2.5. Potential density ($\sigma \theta$) in relation to depth at the station Panulirus.

the continental slope. Colebrook and Taylor (1979) continued Bjerknes' research and found cooling of the north Atlantic sea surface water between 1948 and 1974.

When the standard conventional hydrographic measurements have *not* been followed, the minimum potential vortices (f/ρ) ($\partial r/\partial z$), provide an excellent trace of 18SSW (the association with maximum oxygen is weak because the water mass is near the surface).

Studies undertaken by Jenkins (1982), to measure oxygen, salinity and ^3H - ^3He have been successful in identifying 18SSW. The measurements made in 1977-1978 and 1977-1978 clearly show the change in 18SSW and the information obtained in both periods is consistent with hydrographic data collected at the *Panulirus* station (\sim Lat. $32^\circ 10'$ N Long. $064^\circ 30'$ W; Figs. 2.2 and 2.5).

Between 1954 and 1978 there were four periods that provide conclusive evidence about the salinity, temperature, potential vortices and heat flow of 18SSW.

1. Between 1954 and 1964, there was a "classic" 18SSW that basically agrees with Worthington (1959) with some small variations.
2. Between 1964 and 1972 the 18SSW became progressively more dense and colder; temperature and density values were 17.1°C and 26.6 mg cm^{-3} in 1972.
3. Between 1972 and 1975 there was not a strong formation of 18SSW; Talley and Raymer (1982) concluded that the 18SSW was not produced during these years and only the remains of the 18SSW from 1971 were observed.
4. Between 1975 and 1976 the temperature of the 18SSW rose again to relatively high levels with low density (Leetmaa 1976, Worthington 1977). By 1978 the 18SSW had the same characteristics as during 1954-1974.

The 18SSW enters the Caribbean Sea through several straits:

1. between Cuba and Hispaniola, the Windward Passage;
2. between Hispaniola and Puerto Rico, the Mona Passage;
3. between St. Thomas and Santa Cruz, Virgin Islands, the Anegada-Jüngfern Passage; and,
4. on a smaller scale, between the islands of the Lesser Antilles.

SOUTH ATLANTIC CENTRAL WATER (SACW)

During the expedition of the German oceanographic ship *Meteor* between 1925-1927 (Wüst 1935, 1957) found a layer of salinity (36.3 to 37.3 PSU) in the surface of the tropical Atlantic Ocean, with a thickness less than 150 m, and at the same time, its formation was located at the central part of the great gyres. Defant (1961) described the ocean layers in general terms and designated the subtropical convergence zones in the north Atlantic and the south Atlantic as sources of high salinity water (Fig. 2.4).

SOUTH ATLANTIC

A large, stable cell of high pressure hovers over the tropical marine area of southern hemisphere (between 15° and 30°S) during winter months; precipitation diminishes and average air temperatures drop to 20-22°C near the surface of the high salinity water (Cartas de Haurwitz and Austin 1944). These winter conditions lead to a net increase in evaporation and greater salinity at the sea surface.

EQUATORIAL SUBCURRENT

Recent research suggests that the high salinity surface water that lies in the western tropical south Atlantic is a source of high salinity water in the Equatorial Subcurrent (Metcalf *et al.* 1962, Cochrane 1963, 1965; Metcalf and Stalcup 1967) (Fig. 2.6). As the subcurrent crosses the Equator from the south, part of it moves in an anticyclonic (clockwise) direction, near 2°-5°N, and 45°-50°W (off the Brazilian coast near the mouth of the Amazon River; Fig. 2.7), and flows towards the southwest where it forms the Equatorial Subcurrent (Cochrane 1963, Goulet and Inghman 1971, Vázquez de la Cerda 1988).

In research carried out on cruises of the the R/V *Undaunted* and the R/V *Glacier* in 1966 and 1969 respectively, Goulet and Inghman (1971) observed that the dynamic calculus at 105 m relative to 495 m showed speeds of $>95 \text{ cm seg}^{-1}$. In general, the directions were towards the north and stronger in the high salinity zones ($>37.3 \text{ PSU}$) (Fig. 2.8). Transport at latitude 7°S was 6.9 Sverdrups (Sv).

Two possible trajectories bifurcate from the high salinity water mass. In the first possibility, it moves in an anticyclonic manner directly inside the point of origin of the Equatorial Subcurrent at 6.9 Sv and goes towards the southeast. The second possible trajectory is that it continues to the northeast under and together with the Equatorial Current from the north.

GATE & FGGE

In the first major experiment of the GARP (Global Atmospheric Research Program), GATE (GARP Atlantic Tropical Experiment, 1974), off the Brazilian coasts in the Mexican naval oceanographic ship B/O *Matamoros*, the movement of an anticyclonic gyre towards the northeast and high salinity fluctuations were observed (Vázquez de la Cerda, unpublished data). This observation is a major justification for the work of Yi Chao (1998), who mentioned the displacement of anticyclonic gyres from the equatorial Atlantic to the Caribbean Sea.

Mexico also participated in the FGGE (First GARP Global Experiment) in 1979, with the Mexican naval oceanographic ship B/O *H-02*, together with the Instituto Geofisica de la

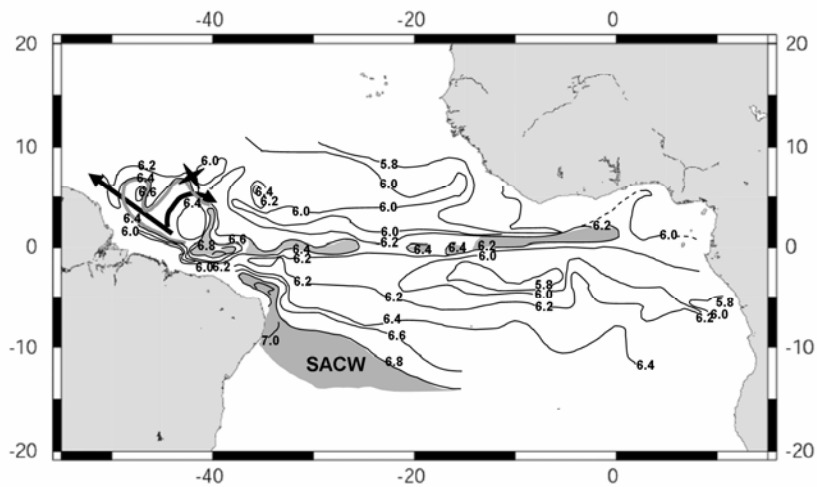


Fig. 2.6. Salinity in the layer of maximum salinity in the equatorial Atlantic Ocean. Equalant I (salinity in psu less than 30 units). Redrawn from Vázquez de la Cerda (1988) modifications of Cochrane (1978).

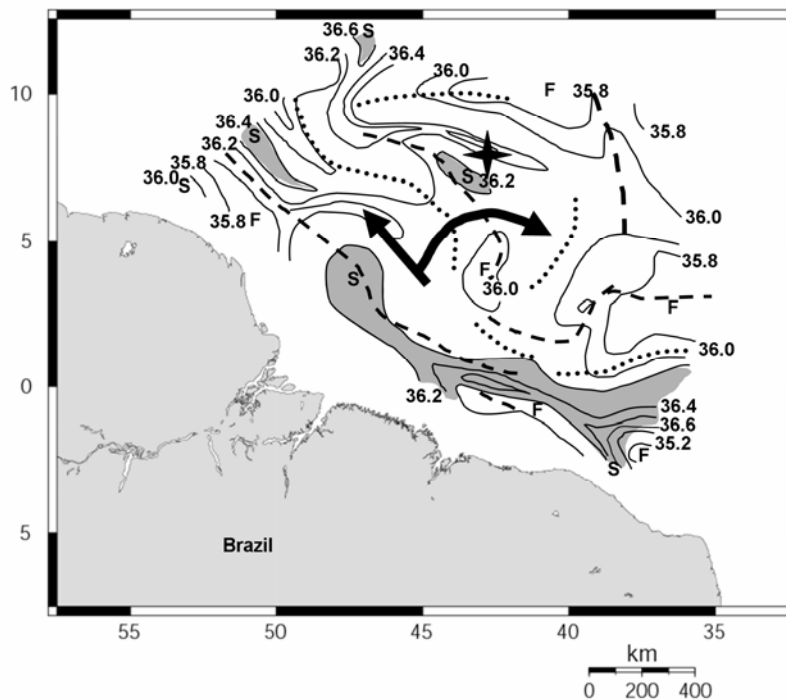


Fig. 2.7. Salinity (PSU) at the surface of the Specific Volume Anomaly ($\delta=240 \times 10^{-8} \text{ m}^3\text{kg}^{-1}$). Data from EQUACHEQUE cruise on board the R/V *Alaminos* (Texas A&M University), July 22-September 11, 1964. Redrawn from Vazquez de la Cerda (1988) modifications of Cochrane (1965). Dotted lines indicate underwater depressions; dashed lines indicate underwater mountain ranges.

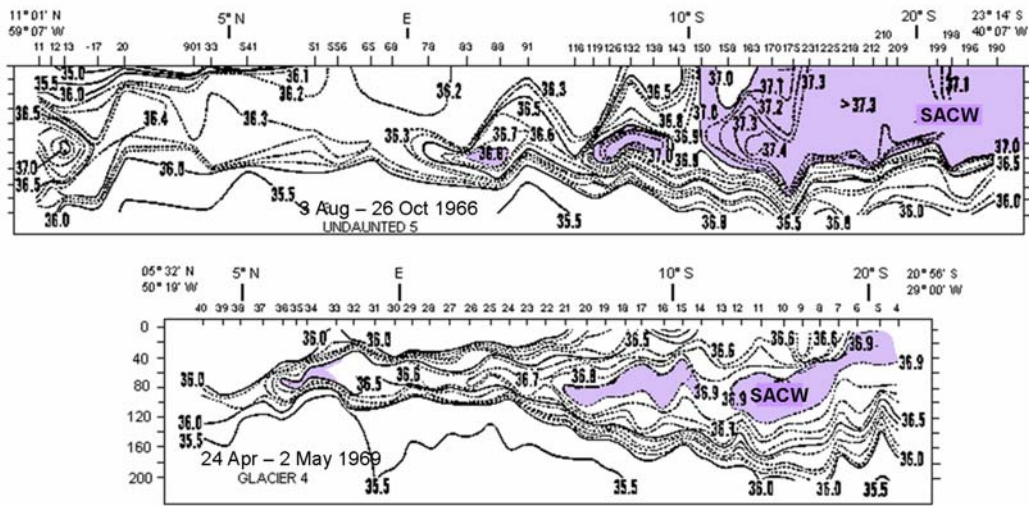


Fig. 2.8. Vertical distribution of salinity (psu) on coast of South America. Upper panel: R/V *Undaunted*, 3 August to 26 October 1966; lower panel, R/V *Glacier*, 24 April to 2 May 1969. From Goulet and Inghman (1971).

Universidad Nacional Autónoma de México (Vázquez de la Cerda 1988). The geographic position of the ship was 7°30' N and 42°30' W during the intensive period of observations (Figs. 2.6, 2.7 and 2.9). A series of oceanographic studies was undertaken every 4 hours from January 26, 1979 to February 20, 1979. During Special Observation Period 1 (Fig. 2.9), from January 25, 1979 to February 19, 1979, maximum salinity values (>36.4 PSU) were always found below the depth the mixing layer. This deepest point for these high salinities was near 140 m on January 28, and closest to the sea surface at 50 m on February 18, which corresponds to the long vertical wave in the thermostructure of ocean waters; this wave registers values near the variations on full moon or new moon tides (every 2 weeks; Fig. 2.10). The highest salinity values were observed every 3 or 4 days. The maximum salinities corresponded to current speeds greater than 40 cm s⁻¹. The highest salinity values (>36.6 PSU), were found at speeds of ~60 cm s⁻¹. During the observation period, transport of the water masses with intermittently high salinity was between 1.9 and 5.6 Sv, with lower values at 4°S; it was thought that the other part had turned towards the east in the Equatorial Subcurrent. Transport estimates for the subcurrent have to be interpreted carefully due to their wide variability over short periods of time.

In the Grenada Straits, Morrison and Nowlin (1982) using data from gathered during Autumn 1973 by the R/V *Caro-I* and stations 2023-2026 sampled by the R/V *Atlantis*, found a cell of high salinity with an estimated value of 1.5 Sv, and a transport value approximately a quarter of the size of that observed off the coast of Brazil (Fig. 2.11).

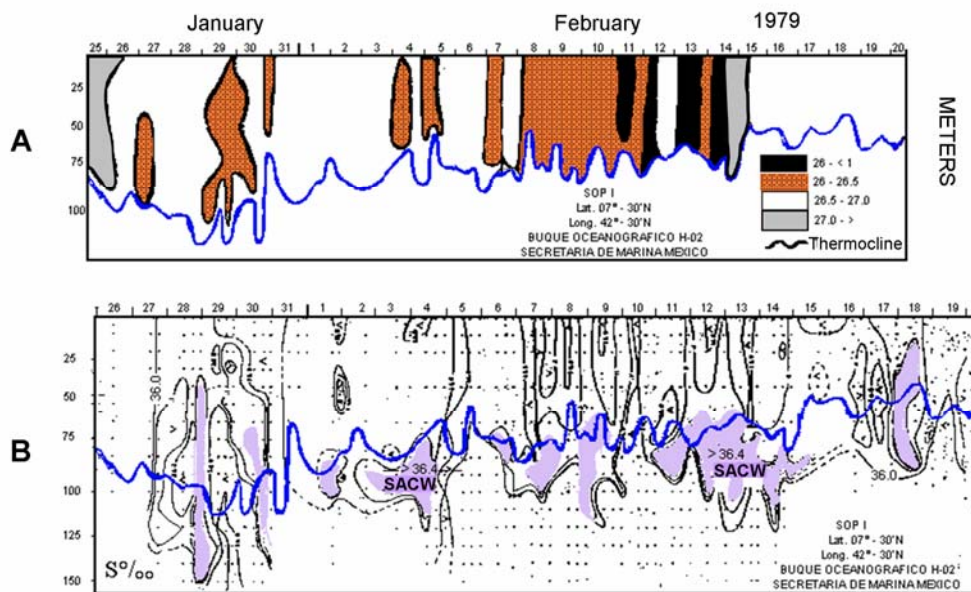


Fig. 2.9. A) Temperature ($^{\circ}\text{C}$) from the surface to 120 m. B) Salinity (psu) from the surface to 160 m deep. Data collected during the Mexican program in the FGGE Oceanographic Ship H-02. Based on Vázquez de la Cerda (1988).

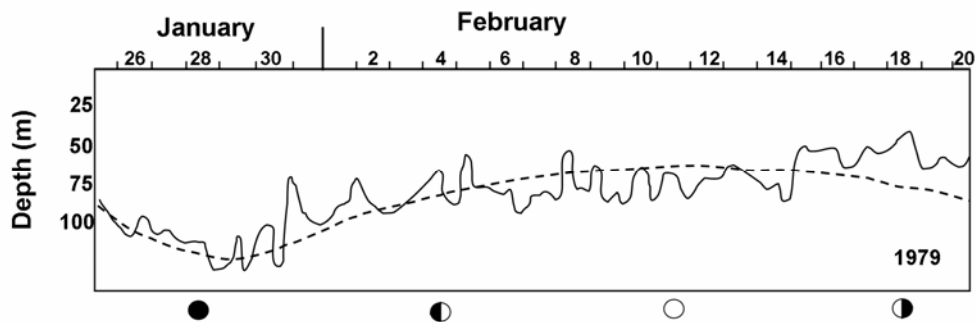


Fig. 2.10. Depth variation (m) occurring at the inception of the thermocline (solid line) in late January at latitude $7^{\circ} 30' \text{N}$ and longitude $42^{\circ} 30' \text{W}$. The average thermocline depth (dashed line) corresponds to the fortnightly tide caused by the new moon and the full moon (correlation coefficient = 0.959)

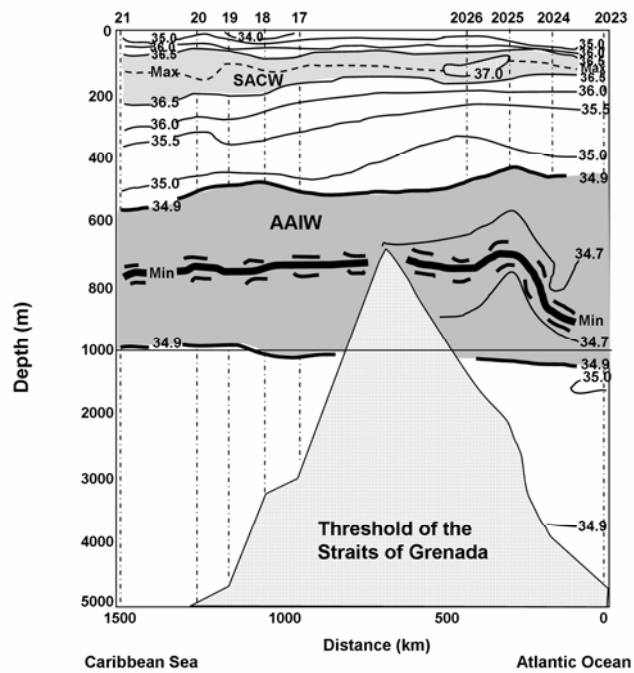


Fig. 2.11. Vertical section of salinity (psu) through the Straits of Grenada, Autumn 1973. Redrawn from Morrison and Nowlin (1982).

ANTARCTIC INTERMEDIATE WATER (AAIW)

DESCRIPTION OF THE REGION

Svedrup (1942) divided the southern part of the oceans into different regions (Fig. 2.12). I also refer to Whitworth's (1980) system of terms in this section.

Near Antarctica, the temperature at the sea surface fluctuates between 1.0-1.5°C below zero and the water remains liquid because of its salinity. However, at a relatively short distance from the coast, the temperature rises slightly to 1-2° C. This region of sudden temperature increase is called the Polar Frontal Zone (PFZ) or Antarctic Convergence, and Deacon (1937) determined from research on the R/V *Discovery* (1932 and 1933) that this is a place where water sinks. As the water continues in a northerly direction, surface temperatures continue to rise slightly until it reaches a second region of rapid temperature increase. This is called the Subtropical Convergence and is near 40° S. The boundary of the Subtropical Convergence is continuous except in the eastern part of the Pacific Ocean or the southern part where it is not well defined. The area that extends from Antarctica to the PFZ is known as the Antarctic Region or Antarctic Zone (AAZ), and the area between the fronts is called the Sub-Antarctic Region or Sub-Antarctic Zone (SAZ). Expeditions during the 1970s led to better definitions for these different regions (Sievers and Nowlin 1984), with the SAZ and the PFZ renamed the Sub-Antarctic Front (SAF).

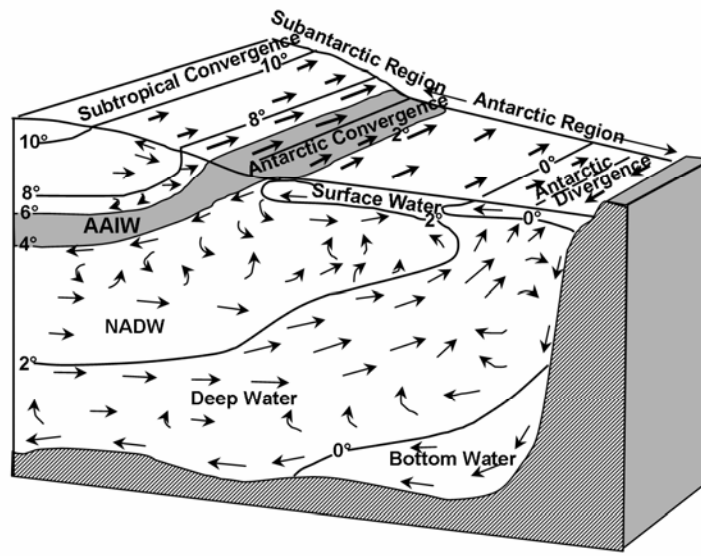


Fig. 2.12. Schematic representation of the currents and water masses in the Antarctic with temperature (°C) distributions. Redrawn from Morrison and Nowlin (1982).

EARLY DEFINITIONS & METHODS

Wüst (1935) used the nucleus method to demonstrate that in the PFZ the nucleus is formed by relatively low salinity water that disperses towards the north alongside the salinity minimum. He called this nucleus the Sub-Antarctic Intermediate Water, but it was later called the Antarctic Intermediate Water (AAIW; Figs. 2.3, 2.11, 2.12 and 2.13a). Although the processes that lead to its formation are not completely understood, Wüst explained that AIA drops to deep levels and moves towards the north. The nucleus method is defined as a region where water parameters are at their maximum or minimum throughout their distribution.

The AAIW includes surface water from AAZ and is formed by a mixture with PFZ waters. It moves in a northerly direction. When it sinks, the AAIW has a width of approximately 300 m, with temperatures from 2-3°C and salinity of 34.2 PSU. The AAIW reaches equilibrium as it travels north where the lower density waters are deeper and the AAIW density ($\sigma_t = 27.4$), sinks. At the same time, the AAIW has relatively high values of dissolved oxygen, 5-7 ml L⁻¹, as a result of having recently left the sea surface (Fig. 2.13c). During its journey to the northern Atlantic Ocean, the salinity of AAIW increases as it mixes and diffuses with adjacent waters. Salinity values throughout its journey are presented in Table 2.1.

Wüst (1964) estimated that less than 5% of the AAIW moves into the Gulf of Mexico. This is confirmed by climatic data collected over several decades and by different cruises. Only small traces of AAIW leave the Gulf of Mexico by the Florida Straits and move toward the North Atlantic by way lower portion of the Gulf Current. On the other hand, the remains of the AAIW journey through the northern and outer portions of the Caribbean Sea next to the Northern Equatorial Current.

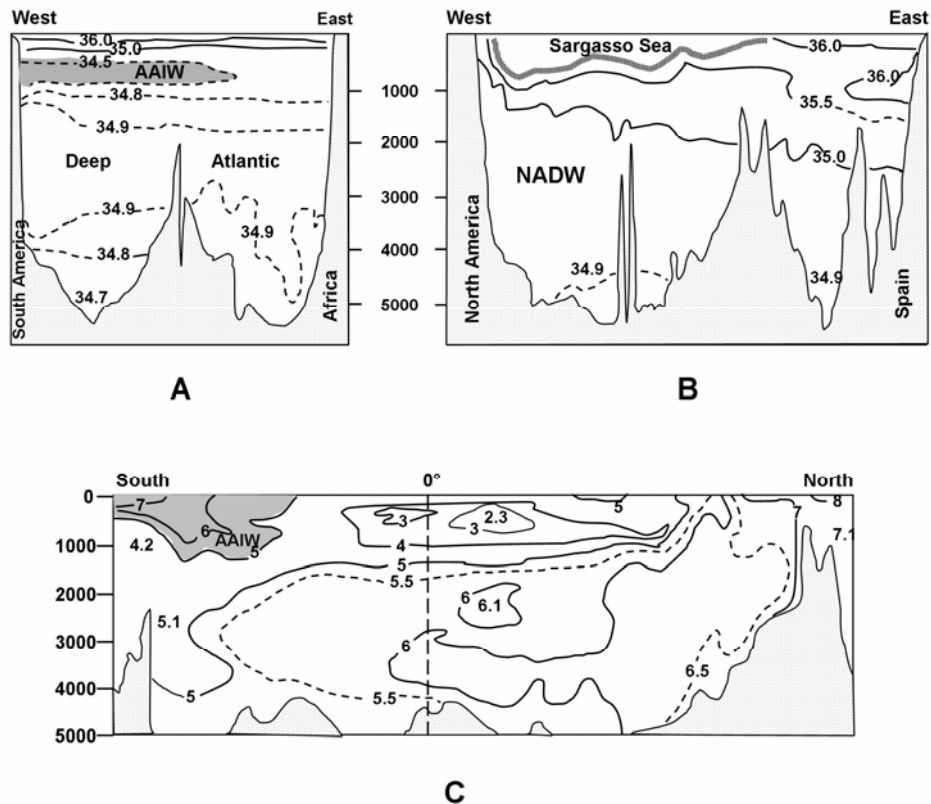


Fig. 2.13. Transects across the Atlantic Ocean showing variations in salinity (PSU; A, B) and dissolved oxygen (ml/L; C). For salinity, transects run from West to East along the 16° South parallel (A) and the 36° North parallel (B). For dissolved oxygen, the transect runs from South to North crossing the equator. Redrawn from GEOSECS Atlas (1976).

Table 2.1. Geographic location Antarctic Intermediate Water (AAIW) of differing salinities between the Antarctic Ocean to the Gulf of Mexico.

PLACE	SALINITY	DEPTH
Argentine Basin	34.2 psu	Surface to >700 m
Brazilian Basin	34.4 psu	700-1,000 m
Equator (0° latitude)	34.5 psu	700-1,000 m
East of the Lesser Antilles	34.7 psu	700-900 m
Eastern Caribbean Sea	34.75 psu	650-850 m
Central Caribbean Sea	>34.80 psu	Between 650 and 850 meters
Yucatan Channel	>34.86 psu	Between 700 and 900 meters.
Central Gulf of Mexico	~34.88 psu	Between 700 and 850 meters

The anticyclonic eddy formed when the AAIW separates from the Loop Current in the eastern Gulf of Mexico is the last dynamic vehicle that will move its remains towards the western Gulf, at depths of 700-1100 m. The AAIW is an important factor in the formation of the anticyclonic gyre and its separation from the main current.

THE CARIBBEAN SEA

The Caribbean Sea is located to the west of the Atlantic Ocean; to the south it is bounded by Central America, Colombia and Venezuela, to the west, Mexico, to the north, the Gulf of Mexico and the Greater Antilles, and the east, the Lesser Antilles. The Caribbean Sea is characterized by being that part of the ocean where the greater part of the Northern Equatorial Current comes together with a parts of the water masses of the Southern Equatorial Current. At the same time the Caribbean Sea receives water masses from the North Atlantic through the main straits (Fig. 2.2), as is explained in the section on 18SSW. Tropical storms, a great number of which become hurricanes, are often spawned in the eastern Caribbean Sea; the energy and the water masses in the sea are changed as they follow the storms along their western trajectories.

The analysis of Cochrane (1968), that synthesizes data from 13 cruises between 1933 and 1972, reveals an oceanic climate in the eastern Gulf of Mexico and to the east of the Caribbean Sea. The Specific Volume Anomaly of 250 cl ton^{-1} is shown in Fig. 2.14, the surface of which corresponds to a density of approximately 25.47 kg m^{-3} (Table 2.2). Table 2.2 also shows the SACW inside rings or gyres and the Common Gulf Water (CGMW) outside new rings; both are characterized by high salinity. However, this surface of 250 cl ton^{-1} can be considered the upper part, and is nearer the sea surface of the 18SSW, with a density of greater than 26.50 kg m^{-3} (Morrison and Merrell 1983).

The analysis undertaken by Cochrane (1968) also clearly shows the entrance of 18SSW resulting from the passage of winds between Cuba and Hispaniola, and through the two straits of the Antilles. Figure 2.14 shows the distinct meeting of the different water masses and particularly the more saline waters in the southeast near the Colombian coast. The meeting of these two water masses; the more saline and warm SACW from the South Atlantic and the less saline water (relative to the SACW) and colder water from the 18SSW on the other, leads to some double diffusion (for an explanation of this phenomenon, see Pond and Pickard 1983, pages 30-31) in the central Caribbean Sea. When these masses of water join the Loop Current through the Yucatan Channel in the eastern Gulf of Mexico, their identity is very subtly preserved as shown by the salinity-depth profiles for the whole Gulf of Mexico, with two salinity maximums that are very close and with very little difference between them (Vázquez de la Cerda and Kelly 1998).

The r and s values, relative density and relative density differences, respectively, are non-dimensional parameters as is the Specific Volume Anomaly. However, in the formulas we have to treat the first two as kg m^{-3} , and, in the case of the Specific Volume Anomaly $10^{-8} \text{ m}^3 \text{ kg}^{-1}$ (to avoid the factor 10 centiliters per ton were used, cl/ton were used previously).

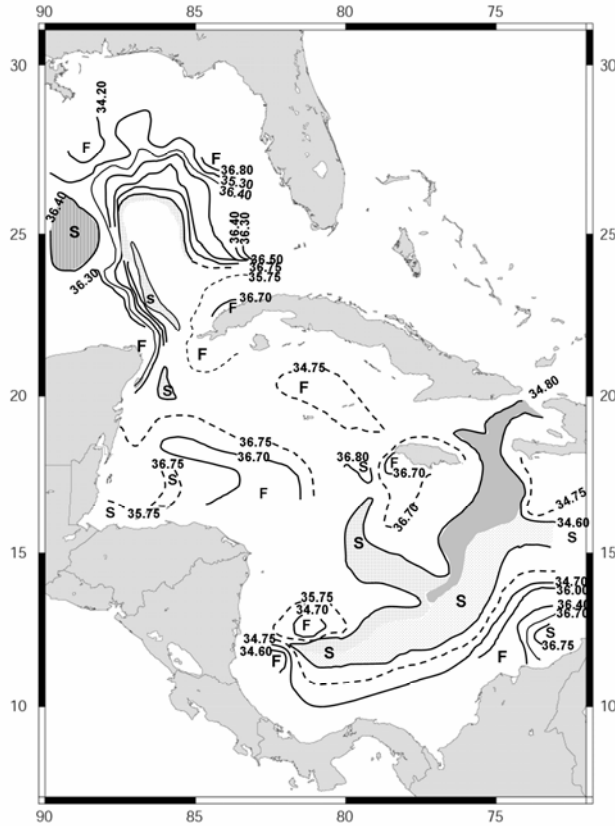


Fig. 2.14. Salinity (psu) at the surface of the Specific Volume Anomaly at 250 cl ton^{-1} from data collected during the 1930s (R/V *Atlantis*, March 1933 and March 1939; R/V *Hannibal*, March 1936), 1958 (R/V *Crawford*), 1960s (R/V *Crawford*, February 1965; R/V *Alaminos*, May 1966 and May 1968), and 1970s (R/V *Alaminos*, February, April, and May 1970, March and April 1972; R/V *Pillsbury*, April 1970). Redrawn from Cochrane (1968).

GULF OF MEXICO

T-S-V DIAGRAM OF THE GULF OF MEXICO

Figure 2.15 presents the water masses in diagram T-S-V (temperature-salinity-volume) in the Gulf of Mexico in February-March 1962 with potential temperature versus salinity (Wilson 1967). Salinity is expressed in Practical Salinity Units (PSU), that correspond exactly to parts per thousand (ppt, ‰), that is to say, the quantity of dissolved salt grams per kilogram of seawater. Research carried out in the 1970s and 1980s show that water masses with a similar distribution behave in the same manner. The numbers in the body of the diagram are multiplied by 1,000 km^3 , and represent the volume of each water mass in the category $2^\circ\text{C} \times 0.2$ of PSU. The sum of the lower part is the potential temperature distribution and to the right is the salinity; the numbers in brackets are the total percentage. The figures in the left-hand margin represent salinity

Table 2.2. Characteristics of the water masses in the Gulf of Mexico. From Morrison and Merrell (1983) modified by Vázquez de la Cerda (1988).

Water Mass	Characteristics	Concentration	Density at S_0 (kg/m^3)	Specific Volume Anomaly $\delta 10^{-8}$ (kg/m^3)	~Depth (m)
<i>Within the Loop Current and new gyres</i>					
SACW	Maximum salinity	36.7-36.8 PSU	25.40	256	150-250
18SSW	Maximum dissolved oxygen	3.6-3.8 ml/L	26.50	150	200-400
<i>Outside the Loop Current and new gyres</i>					
CGMW	Maximum salinity	36.4-36.5 PSU	25.40	256	0-250
<i>Extensions of the Gulf of Mexico</i>					
<i>Tropical</i>					
Central water	Minimum dissolved oxygen	2.5-3.3 ml/L	27.15	90	300-500
Atlantic water	Minimum nitrate	29-25 mg/L	27.30	77	500-700
<i>Antarctica</i>					
AAIW	Maximum phosphate	1.7-2.5 mg/L	27.40	67	600-800
	Minimum salinity	34.88-34.89 PSU	27.50	58	700-1000
CSW	Maximum silicate	23-28 mg/L	27.70	39	1000-1200

between 33 and 37 PSU, and the figures along the upper margin represent the temperature in Celsius.

Figure 2.15 shows the T-S-V diagram, as well as the curves of equal density with values in the levels (kg m^{-3}) in the upper part, and on the same lines, in the lower part, the Specific Volume Anomaly ($d = 10^{-8} \text{ m}^3 \text{ kg}^{-1}$). At the same time there are six ellipses that approximately delimit the different water masses. The values between brackets inside each ellipse are shown in Table 2.3, and only indicate the percentages of water masses in the Gulf of Mexico.

The water masses that come from the Atlantic Ocean, from the north, the 18SSW, and from the south the SACS, are mainly characterized by maximum salinity. Cochrane (1968), in his analysis of the Specific Volume Anomaly ($d = 250 \times 10^{-8} \text{ m}^{-3} \text{ kg}^{-1}$) in the Caribbean Sea clearly shows the meeting between two water masses in the central part of this Sea (Fig. 2.14), whose depth varies between 150 and 250 m, which is where maximum salinity is located. This region where the water masses unite has undergone double diffusion, before the masses enter the Gulf of Mexico.

The 18SSW and the SACW have approximately similar salinity values and it is very probable that the double diffusion phenomenon, called “salt fingers” exists in the central part of the Caribbean Sea, although until now this phenomenon has not been reported. In addition, there are two salinity maximums in many of the oceanographic stations for the depth-salinity profiles inside the Gulf of Mexico. These are close to each other and the variation between them is very small.

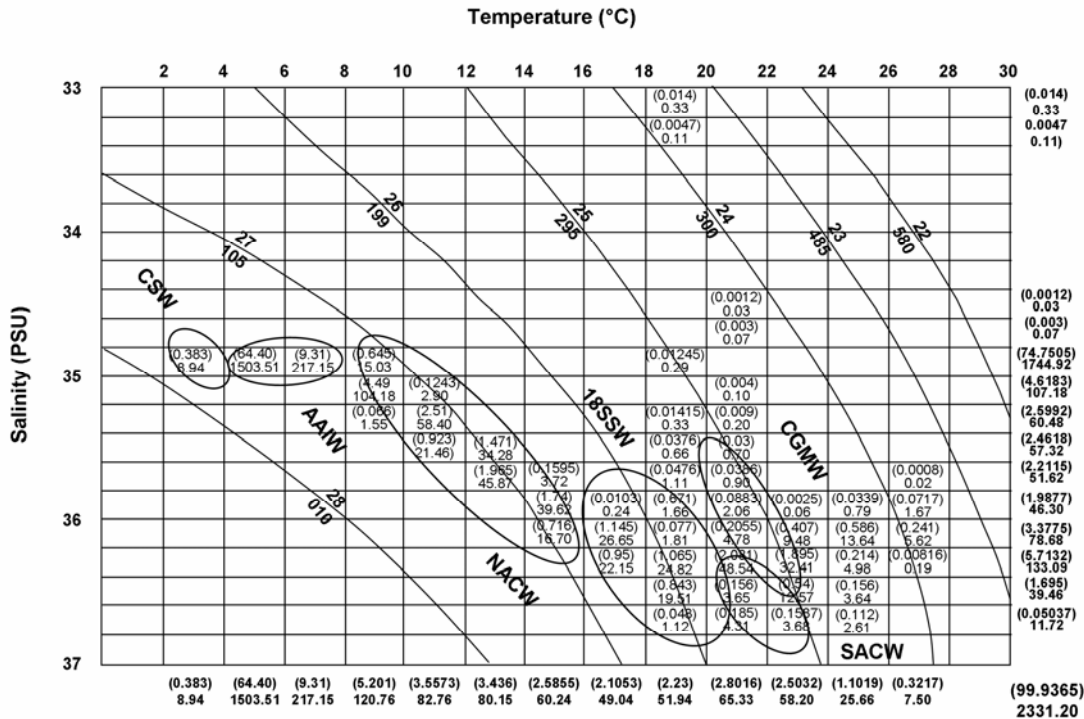


Fig. 2.15. Temperature-Salinity-Volume (T-S-V) diagram of the Gulf of Mexico. The ellipses delineate the different water masses. From Wilson (1967) modified by Vázquez de la Cerda (1998).

Table 2.3. Percentages of water masses in the Gulf of Mexico.

Water mass	Percent
SACW	1.24
CGMW	4.83
18SSW	3.72
NACW	14.58
AAIW	73.71
CSW	0.38
Total	98.46

OCEAN CHARACTERISTICS OF THE GULF OF MEXICO

Large anticyclonic rings break off from the Loop Current at intervals of 6-17 months (Ichiye 1962, Cochran 1972, Behringer *et al.* 1977, Elliott 1982, Vukovich and Crissman 1986) and, as their name suggests, their rotation is clockwise. These rings break off towards the west in the deep part of the Gulf of Mexico at a translation speed of 1-4 km/day (Elliott 1982, Vukovich and Crissman 1986). Their diameter is about 300 km and their movement affects dynamics of

water masses at depths greater than 3,000 m (Kelly *et al.* 1987). The upper water masses in the central part of the Gulf of Mexico are relatively warmer and more saline, with salinities above 36.5 PSU, (Nowlin 1972, Vázquez de la Cerda 1975), and their transport is between 10 and 12 Sv (Vázquez de la Cerda 1975). During their movement towards the west of the Gulf the anticyclonic rings generate large cyclonic rings and transfer potential and kinetic energy (Reid personal communication, Merrell and Morrison 1981, Merrell and Vázquez 1983). The most notable large cyclonic rings are those found on the continental shelf of Texas (Cochrane and Kelly 1986) and those in the western part of the Campeche Bay to the southeast of the Gulf of Mexico (Nowlin 1972, Vázquez de la Cerda 1975, 1993). Another, smaller and recurrent cyclonic ring is located to the northeast of the Laguna Tamiahua (Vázquez de la Cerda 1975, Vidal *et al.* 1992). The characteristics of cyclonic rings are: diameter = <200 km; zone of influence = <1000 m depth; water masses in the central upper part of the ring are cooler, due to the swell caused by their counterclockwise circulation; and sometimes deeper ventilation in the isotherm layers.

As the anticyclonic ring moves towards the west it transfers energy and it is extended due to submarine topography; the most notable case of this is found in the Cañon de Campeche in the deep limit of the western continental shelf of Campeche Bay. The extension over the Cañon de Campeche is called a current intrusion (Vázquez de la Cerda 1975) and sometimes this current is found off the coast of the Tuxtlas, Veracruz, and during winter as a result of cold fronts, known locally as “Nortes,” and they form a double orthogonal ground swell that is very dangerous for navigation.

In Campeche Bay, the cyclonic ring has a water transport of 3.3 ± 1.8 Sv (Vázquez de la Cerda 1993). Its variation depends a lot on the affect produced by cold fronts during the autumn and winter (Blaħa and Sturges, 1981), and the intrusion current correlation is very high.

The relation between intrusion current and cyclonic ring is inversely proportional: when the intrusion current is extensive and deep the cyclonic ring is small, and when the cyclonic ring covers most of Campeche Bay, the intrusion current is small (Vázquez de la Cerda 1993). This relationship has been shown from analysis of data collected during 20 cruises in the southeastern Gulf of Mexico over 40 years.

Analysis of circulation on the Texas-Louisiana slope, based on the elevation of the sea surface and the speed fields using the geopotential anomaly, shows variation of the anticyclonic and cyclonic rings in the northeastern Gulf of Mexico between 1992 and 1994 (Jochens 1997). This is the area where energy dissipation and deformation of the anticyclonic rings begins.

When the anticyclonic rings in the Gulf of Mexico are off the coasts of Tamaulipas, they start to get longer, form of ellipses and dissipate to form cyclonic rings (Merrell and Morrison 1981, Merrell and Vázquez 1983). Figure 2.16 shows data obtained during the *Cosma 7122* cruise. The central part of the ring has the remains of the maximum salinity values of the 18SSW from the north, and the SACW from the south, although it is probable that the quantity of SACW water is very small.

The distribution of AAIW in the Gulf of Mexico is shown in Fig. 2.17. It is found in the Loop Current in the eastern Gulf with depths greater than 850 m and with salinity values that fluctuate upwards from 34.86 PSU higher and in the western Gulf where depths are from 750 m and deeper, with salinities from 34.88-34.89 PSU (Nowlin 1972).

The transect A-B in Fig. 2.18, between the continental shelf off the Port of Tampico and the continental shelf off Campeche, on latitude 22°20'N from data collected during the *Cosma 71-10* cruise in May-June 1971 gives an excellent view of the vertical cross-section of an

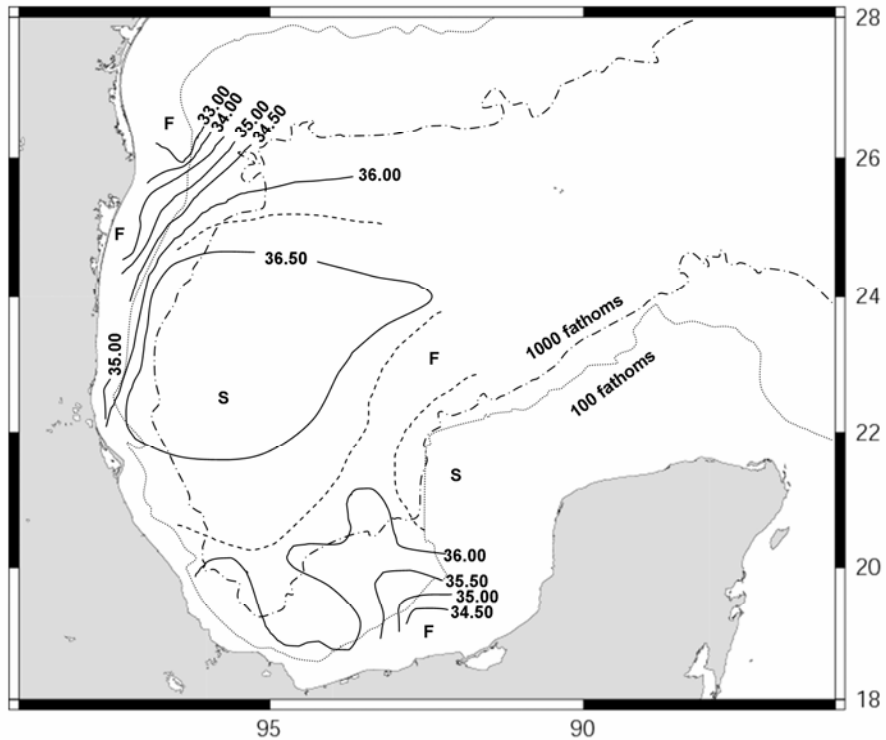


Fig. 2.16. Surface salinity (psu) observed in November 1971 (Cosma 71-22). Redrawn from Vázquez de la Cerda (1975).

anticyclonic ring. Although many cruises have taken place since then, this A-B transect clearly shows the cross-section of all the characteristics of the different water masses, the thermostructure and the salinity of the anticyclonic ring. In the first 100 m of depth the 18SSW and SACW are found, with a quantity of $15,760 \text{ km}^3$, that is to say 17.2%. Then, between 100 and 500 m depth the North Atlantic Central Water (NACW) water mass is found in the form of an inverted cone, with a quantity of $20,800 \text{ km}^3$ and a percentage of 22.7%. Finally, the AAIW is divided in parts, between 550 and 850 m depth, corresponding to maximum phosphates in the form of an inverted mushroom; and deeper, between 850 and 1200 m depth, corresponding to minimum salinity in an almost circular form. The vertical and horizontal are really extended revolving ellipses due to differences in scale; the total volume of AAIW is $55,000 \text{ km}^3$, or 60%. Although the values are approximate, they are consistent with the percentages given by Wilson (1967), when the fact that they refer to the whole Gulf of Mexico is taken into account.

The AAIW, as well as having the greatest percentage in the diagram elaborated by Wilson (1967) and the transect mentioned above, has salinity values of 34.82 PSU in the nucleus of the water mass, that must correspond to the normal values found the eastern Caribbean Sea (see Table 2.1). If these two characteristics, the greater percentage and lower salinity values in the nucleus, are always consistent, then the AAIW will be the most important factor in the separation of anticyclonic rings from the Loop Current. It has not been possible to prove lower salinity values in the nucleus of another anticyclonic ring again.

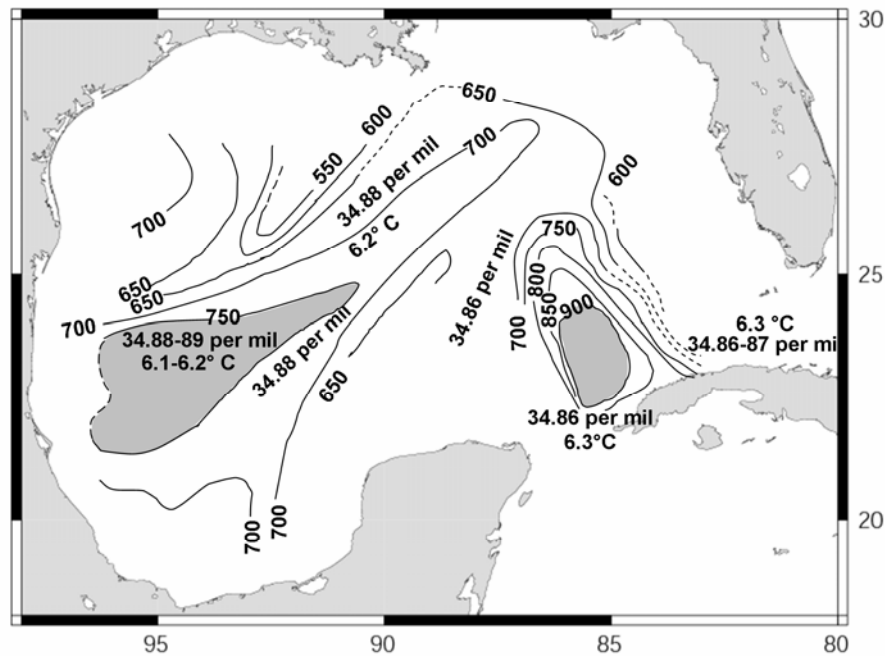


Fig. 2.17. AAIW in the Gulf of Mexico during 1962. Depth (50 m intervals) of the remnant of the AAIW (minimum salinity). Data collected during the Hidalgo 62-H-3 cruise. Redrawn from Nowlin (1972).

The threshold of the Yucatan Straits is 2,040 m and the depth of the Florida Strait is slightly more, at 900 m. This is why the AAIW can penetrate the Gulf of Mexico without difficulty, but its departure is minimum and due only to the drag of the upper water masses. That is to say, the AAIW accumulates at the entrance of the Gulf of Mexico and this largely accounts for the extension of the Loop Current. The separation of the anticyclonic rings that occurs in the current later is produced when the volume of water of the nucleus of the AAIW has increased considerably and breaks the dynamic equilibrium of the whole column of water, provoking the extension of cyclonic meanders from the continental shelf of the Yucatan and Florida (Cochrane 1972).

DISCUSSION AND CONCLUSIONS

Research has recently intensified on areas of deep water in the Gulf of Mexico in order to obtain more data and to improve existing mathematical models.

The qualitative aspects of the formation of anticyclonic rings in the Loop Current in the eastern Gulf of Mexico are well known. At the same time, the locations of the mostly permanent cyclonic rings in the Gulf are also known. The first is located in the extreme east off the western coast of the Florida peninsula, the second covers the entire continental shelf off the Texas coast, the third is found in Campeche Bay; and the fourth is a recurrent gyre in northeast of Laguna Tamiahua in northern Veracruz.

The most important phenomenon in the Gulf of Mexico is the formation of anticyclonic rings that separate from the Loop Current; the interval of separation varies from months to more

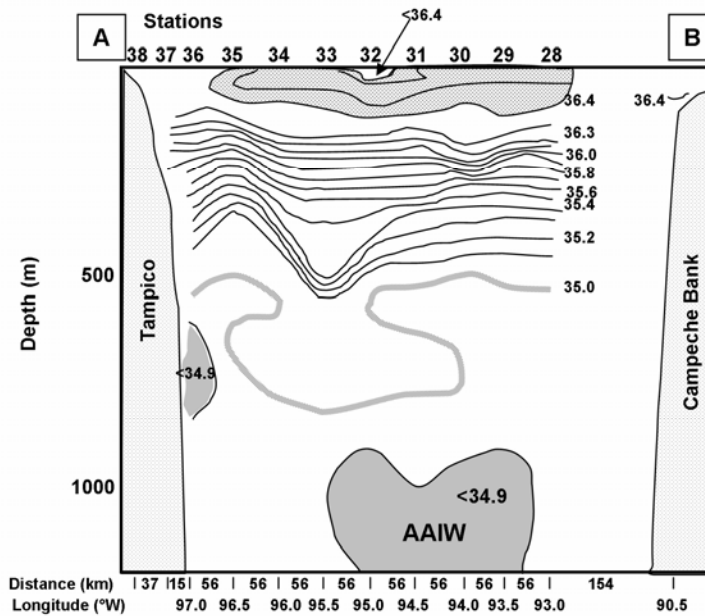


Fig. 2.18. Salinity (psu) along a vertical transect, May-June 1971 (COSMA 71-10). Vertical exaggeration 500:1. Redrawn from Vázquez de la Cerda (1975).

than a year, with an average of 10 months (Sturges and Leben 2000). These rings break away to the west of the deepest part of the Gulf. The large anticyclonic ring that separates from the Loop Current, and that carries the water masses from different regions of the Atlantic Ocean, the 18SSW, the SACW, and the AAIW, will be the region with the highest temperature and salinity. The geopotential of this anticyclonic ring will be transferred to the before-mentioned cyclonic rings and will form part of the Common Gulf Water (CGMW) due to mixing and diffusion.

The formation of the three water masses in the different regions of the Atlantic ocean is mainly due to the cooling of the sea surface due to atmospheric cold fronts and, as a consequence, water density increases and sinks until it reaches equilibrium. The SACW is shallower and saltier than the 18SSW of the northern Atlantic. When they meet in the central Caribbean Sea they produce double diffusion and at the entrance to the Gulf of Mexico they are found in the upper part of the Loop Current. Lastly, the AAIW that is formed between the Antarctic polar fronts is the deepest and its greater volume leads to the formation of the Loop Current. The respective volumes of the three water masses contribute to intermittent pulsations.

The formation of anticyclonic gyres near the equator and their movement to the northeast, together the North Equatorial Current (NEC), bring with them water masses from the southern hemisphere. These gyres, while moving through the Caribbean Sea, contribute to the formation of the Loop Current.

We consider that the formation of the Loop Current is through the transfer of eddies and the movement of the three water masses, where the AAIW is the most important. Because the AAIW does not leave the Gulf of Mexico, it causes dynamic disequilibria by initiating an

anticyclonic turn that reaches the depth of the Loop Current, causing formation of anticyclonic rings in the eastern Gulf of Mexico.

DEDICATION

This work is dedicated to Professor John D. Cochrane and Dr. Takashi Ichiye, who were my mentors and teachers during my master's work at Texas A&M University, College Station (1973-1975). It is also dedicated to admirals Antonio Vázquez del Mercado and Gilberto Lopez Lira of the Secretaría de Marina, both scientists and sailors who both promoted and contributed greatly to oceanographic knowledge of the Gulf of Mexico. Their memory will be a greatly encourage future research into the seas.

ACKNOWLEDGEMENTS

To Dr. George L. Huebner and Professor Robert O. Reid of Texas A&M University for their great patience and guidance during my doctorate and professional development. To Dr. Ingvar Emilsson, a great teacher, friend and pioneer of Mexican physical oceanography. To Dr. Bonifacio A. Pena Pardo of the Instituto de Ingeniería and the Universidad Veracruzana for their great support. To Engineer Juan Carlos Gutierrez Quevedo for his help in the production and completion of this document. Partial financing came from the Universidad Veracruzana, Proyecto No. R 272106.

LITERATURE CITED

- Blaha, J. P. and W. A. Sturges. 1981. Evidence for wind-forced circulation in the Gulf of Mexico. *Journal of Marine Research* 39:711-734.
- Behringer, D. W., R. L. Molinari and J. F. Festa. 1977. The variability of anticyclonic current patterns in the Gulf of Mexico. *Journal of Geophysical Research* 82:5469-5476.
- Bjerknes, J. 1964. Atlantic air-sea interaction. *Advances in Geophysics* 10:1-82.
- Chao, Y. 1998. Mesoscale eddies in the Caribbean Sea. In *U.S. WOCE Implementation Report Number 10, August 1998*. College Station: U.S. WOCE Office.
- Cochrane, J. D. 1963. Equatorial undercurrent and related currents off Brazil in March and April 1963. *Science* 142:669-671.
- 1965. Equatorial currents of the western Atlantic. Department of Oceanography Program Report Reference 65-T. College Station: Texas A&M University.
- 1968. Currents and waters of the eastern Gulf of Mexico and western Caribbean, of the western tropical Atlantic Ocean, and of the eastern tropical Pacific Ocean. Department of Oceanography Program Report Reference 68-8T. College Station: Texas A&M University.
- 1972. Separation of an anticyclone and subsequent development in the Loop Current during 1969. Pp. 91-106 in L. R. A. Capurro and J. L. Reid (eds.), *Contributions on the Physical Oceanography of the Gulf of Mexico*. Houston: Gulf Publishing Co.
- Cochrane, J. D. and F. J. Kelly 1986. Low-frequency circulation on the Texas-Louisiana continental shelf. *Journal of Geophysical Research* 9:10645-10659.

- Colebrook, J. M. and A. H. Taylor 1979. Year-to-year changes in sea-surface temperatures, North Atlantic and North Sea, 1948 to 1974. *Deep-Sea Research Part A. Oceanographic Research Papers* 26: 825-850.
- Deacon, G. E. R. 1937. The hydrology of the Southern Ocean. *Discovery Reports* 15:1-24.
- Defant, A. 1961. *Physical Oceanography*. New York: Pergamon Press. 2 volumes.
- Elliott, B. A. 1982. Anticyclonic rings in the Gulf of Mexico. *Journal of Physical Oceanography* 12:1292-1309.
- Goulet, J. R. Jr, and M. C. Ingham. 1971. The shallow layer of high salinity in the southwestern Tropical Atlantic Ocean. *Bulletin of Marine Science* 21:716-732.
- Haurwitz, B. and J. M. Austin. 1944. *Climatology*. New York: McGraw-Hill. 410 pp.
- Ichiye, T. 1962. Circulation and water mass distribution in the Gulf of Mexico. *Geofísica. Internacional* 2:47-76.
- Jenkins, W. J. 1982. On the climate of a subtropical gyre: decade time scale variations in water mass renewal in the Sargasso Sea. *Journal of Marine Research* 40 (Supplement): 265-290.
- Jochens, A. E. 1997. Circulation over the Texas-Louisiana slope based on sea surface elevation and current velocity fields. Ph.D. dissertation, Texas A&M University, College Station. 145 pp.
- Kelly, F. J., A. M. Vázquez and D. A. Brooks. 1987. El origen de los remolinos oceánicos en la frontera entre U.S.A. and Mexico. In *Memoria II Reunión Indicativa de Actividades Regionales Relacionadas con la Oceanografía (Noviembre de 1987)*. Veracruz, México: Comisión Intersecretarial de Investigación Oceanográfica.
- Leetmaa, A. 1977. Effects of the winter of 1976-1977 on the northwestern Sargasso Sea. *Science* 198:188-189.
- Merrell, W. J., Jr. and J. M. Morrison 1981. On the circulation of the western Gulf of Mexico with observations from April 1978. *Journal Geophysical Research* 86:4181-4185.
- Merrell, W.J. Jr. and A. M. Vázquez. 1983. Observations of changing mesoscale circulation patterns in the western Gulf of Mexico. *Journal Geophysical Research* 88:7721-7723.
- Metcalf, W. G., A. D. Voorhis and M. C. Stalcup. 1962. Origin of the Atlantic Equatorial Undercurrent. *Journal Geophysical Research* 67:2499-2508.
- Metcalf, W.G. and M. C. Stalcup. 1967. Origin of the Atlantic Equatorial Undercurrent. *Journal Geophysical Research* 72:4959-4975.
- Morrison, J. M. and W. D. Nowlin. 1982. General distribution of water masses within the eastern Caribbean Sea during the winter of 1972 and fall of 1973. *Journal Geophysical Research* 87: 4207-4229.
- Morrison, J. M. and Merrell W.J. 1983. Property distributions and deep chemical measurements within the western Gulf of Mexico. *Journal Geophysical Research* 88:260-2602.
- Nowlin, W. D., Jr. 1971. Winter circulation patterns and property distributions. Pp. 3-53 in L. R. A. Capurro and J. L Reid (eds.), *Contributions on the Physical Oceanography of the Gulf of Mexico*. Houston: Gulf Publishing Co.
- Pond S. and G. L Pickard. 1983. *Introductory Dynamical Oceanography*. Pergamon Press: Oxford. 329 pp.
- Sievers, H. A. and W. D. Nowlin, Jr. 1984. The stratification and water masses at Drake Passage. *Journal Geophysical Research* 89:10489-10514.

- Sturges, W. and R. Leben 2000. Frequency of ring separations from the Loop Current in the Gulf of Mexico: a revised estimate. *Journal Physical Oceanography* 30:1814-1819.
- Sverdrup, H.U., M.W. Johnson and R. H Fleming. 1942. *The Oceans, their Physics, Chemistry, and General Biology*. New York: Prentice-Hall, Inc. 1087 pp.
- Talley, L. D. and M. E. Raymer. 1982. Eighteen degree water variability. *Journal of Marine Research* 40:757-775.
- Vázquez de la Cerda, A. M. 1975. Currents and Waters of the Upper 1200 m of the Southwestern Gulf of Mexico. M.S. thesis, Texas A&M University, College Station. 108 pp.
- 1988. Some oceanographic results in the western Equatorial Atlantic Ocean and their consequences in the Gulf of Mexico. Texas A&M University Oceanography Seminar, October 24 – October 28, 1988. College Station, Texas.
- 1993. Bay of Campeche Cyclone. Ph.D. dissertation, Texas A&M University, College Station. 91 pp.
- and F. J. Kelly. 1998. Desarrollo del remolino Fourchon (1998) en el Golfo de México. Abstract in *V Congreso Nacional de Ciencias y Tecnologías del Mar, November 12-14, 1998*. Boca del Río, Veracruz, Mexico.
- Vidal, V. M., F. V. Vidal and J. M. Pérez-Molero. 1992. Collision of Loop Current anticyclonic ring against the continental slope of the western Gulf of Mexico. *Journal Geophysical Research* 97:2155-2172.
- Vukovich, F. M. and B. W. Crissman. 1986. Aspects of warm rings in the Gulf of Mexico. *Journal Geophysical Research* 91:2645-2660.
- Whitworth, T., III. 1980. Zonation and geostrophic flow of the Antarctic Circumpolar Current at Drake Passage. *Deep-Sea Research* 27A: 497-507.
- Wilson, R. J. 1967. Amount and Distribution of Water Masses in February and March 1962 in the Gulf of Mexico. M.S. thesis, Texas A&M University, College Station. 54 pp.
- Worthington, L.V. 1959. The 18° Water in the Sargasso Sea. *Deep-Sea Research* 5:297-305.
- 1977. The intensification of the Gulf Stream after the winter of 1976-1977. *Nature* 270:415-417.
- Wüst, G. 1935. Schichtung und Zirkulation des Atlantischen Ozeans: Die Stratosphäre. Pp. 109-228 in, *Wissenschaftliche Ergebnisse der Deutschen Atlantischen Expedition auf dem Forschungs-und Vermessungsschiff Meteor, 1925-1927, Band VI, Erster Teil*. Berlin: Alter de Gruyter. (The Stratosphere of the Atlantic Ocean, W. J. Emery (ed.), 1978. New Delhi: Amerind. 112 pp).
- . 1957. Stromgeschwindigkeiten und Strommgen in derTiefen des Atlantischen Ozeans. Pp. 261-420 in *Wissenschaftliche Ergebnisse der Deutschen Atlantischen Expedition auf dem Forschungs-und Vermessungsschiff Meteor, 1925-1927, Band VI, Zweiter Teil*. Berlin: Alter de Gruyter
- . 1964. *Stratification and Circulation in the Antilles-Caribbean Basins*. New York: Columbia Univ. Press. 201 pp.

TERMINOLOGY

ml l^{-1} – corresponds to milliliters per liter ($1 \text{ ml} = 10^{-3}$ liter).

mg-at l^{-1} – corresponds to micrograms-atom per liter ($\mu\text{g} = 10^{-6}$ grams).

Ocean station – when an investigation ship stops and remains adrift to undertake measurements of several parameters at different depths.

Potential vorticity – the product of static stability and absolute vorticity that conserved in a adiabatic (no heat lost or gained) flow. Absolute vorticity is a kinematic characteristic of flow that expresses its tendency to move. Planetary vorticity or Coriolis parameter, $f = 2\Omega \sin\phi$; ($\Omega = 7.29 * 10^{-5}$ rad/s).

PSU (Practical Salinity Unit) – quantity of dissolved grams of salts in a kilogram of seawater (gr kg^{-1} or ‰ or ppt).

σ – the symbol called *sigma-t*, an abbreviated annotation to indicate the density of a sample of seawater, using the relation $\text{sigma-t} = (\text{density} - 1) * 10$, in such a way that normal seawater, whose density is 1.02680, has a sigma-t of 26.8.

Specific Volume Anomaly – previously expressed in centiliters ton (cl ton^{-1}) in order to avoid the coefficient 10^{-8} when expressing it in $\text{cm}^3 \text{ gr}^{-1}$.

Sverdrup (Sv) – a unit of transport or effort = $10^6 \text{ m}^3 \text{ s}^{-1}$ = one million cubic meters per second.

Thermocline – the strata of water in which a marked vertical temperature gradient is observed.